

209. Linear-reactor-infrared-matrix and Microwave Spectroscopy of the *cis*-2-Butene Gas-phase Ozonolysis

by Heinz Kühne, Martin Forster, Jürg Hulliger, Heidi Ruprecht, Alfred Bauder and Hans-Heinrich Günthard¹⁾

Laboratory for Physical Chemistry, ETHZ, CH-8092 Zurich

(23.VI.80)

Summary

Investigation of the formation of complex products in the gas-phase ozonolysis of *cis*-2-butene by linear-reactor-infrared-matrix and linear-reactor-microwave spectroscopy is reported. The following species have been unequivocally detected: secondary 2-butene ozonide, acetic acid, peracetic acid, glycolaldehyde, dimethyl ketene, the simple and mixed anhydrides of formic and acetic acid, 2,3-epoxybutane and 2-butanone, besides polyatomic products already known. In contrast, the primary ozonide has been detectable neither by LR-MW. nor by LR-IR. Observation of both stereoisomeric epoxides and kinetic modelling are used to support the intermediate formation of the *O'Neal-Blumstein* radical $\text{CH}_3\text{CH}(\text{O}_2)\text{CH}(\text{O})\text{CH}_3$ and the existence of a reaction channel in which the two carbon atoms of the C,C double bond of the olefin remain connected. As the dominant reaction path a mechanism with a *Criegee* type split into methyldioxirane (ethylidene peroxide) and acetaldehyde is considered and subsequently proposed to explain formation of many complex products by either unimolecular or bimolecular processes of the peroxide. For the reactions considered, thermochemical estimates of reaction enthalpies and activation data are included. Kinetic modelling for a partial reaction mechanism involving at least two different paths of decay of the *O'Neal-Blumstein* biradical into *Criegee*-type intermediates and the 2,3-epoxybutanes is discussed.

1. Introduction. – Kinetics and mechanism of the ozonolysis of *cis*-2-butene have been the subject of rather intense research work. Product analysis and relative rate studies have been reported by *Cvetanovic et al.* [1] [2] as early as 1963. Though acetaldehyde was detected among the products, acetic acid was apparently not found. Instead considerable amounts of formic acid and traces of propene were detected. From chemiluminescence studies *Finlayson et al.* [3] inferred the existence of vibrationally excited OH among the reaction products. By observing the IR. spectra of the reaction mixture in the solid state after reaction of

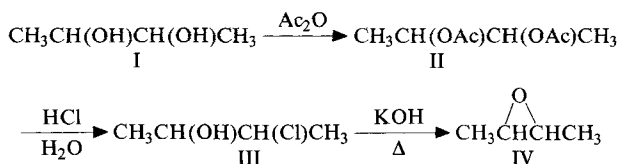
¹⁾ Author to whom correspondence should be addressed.

O₃ with *cis*-2-butene at -160 to -182° , *Heicklen et al.* [4] claimed to have detected the primary ozonide of *cis*-2-butene. In a photoionization low-resolution mass-spectroscopy study by *Atkinson et al.* [5] [6] of the *cis*-2-butene/ozone-gas-phase reaction at 2 Torr total pressure, formation of formaldehyde, methanol, hydrogen peroxide, ketene, acetaldehyde, formic acid and glyoxal was inferred from mass spectra, besides a number of radical species like formyl, hydroperoxyl, hydroxyethyl (CH₂OHCH₂). Based on low resolution mass spectra a large number of complex-reaction products were tentatively considered. The same authors gave mass-spectroscopic and gas-chromatographic evidence for the production of 2-butanone and 3-buten-2-one from *cis*-2-butene ozonolysis in the presence of O₂. In view of these results they gave preference to the *O'Neal-Blumstein* mechanism [7]. *Huie & Herron* using a stopped-flow/photoionization mass-spectroscopy technique derived values for the rate constant of the ozone/*cis*-2-butene reaction [8]. These authors carried out extensive kinetic modelling studies with the aim to reproduce the observed time behavior of the main products from ethene, propene and 2-methyl-1-propene ozonolysis, but no attention was given to possible complex reaction products [9] [10].

Investigation of the *cis*-2-butene/ozone-gas-phase reaction in the presence of formaldehyde by IR. Fourier transform spectroscopy by *Niki et al.* [11] allowed the identification of the secondary propene ozonide among the products, in particular methane, formic acid and methanol. Surprisingly neither acetic acid nor secondary butene ozonides were detected. This observation seems to support the *Criegee* mechanism [12]. By application of linear-reactor-infrared-matrix and microwave spectroscopy to the ethylene-gas-phase ozonolysis *Kühne et al.* [13] proved independently the *Criegee* mechanism to be the dominant reaction channel. However, these authors showed that there exists a second mechanism of smaller efficiency in which the two C-atoms of the C,C double bond remain connected. Furthermore, it was demonstrated that ethylene ozonolysis leads to complex products like formic acid anhydride and glycolaldehyde, which contain all but one or two C-atoms of the initial reactants. On the other hand neither primary nor secondary ethylene ozonide was detectable among the products of the homogeneous gas reaction.

In this paper we report a study of the gas-phase ozonolysis of *cis*-2-butene by combination of the linear reactor with infrared-matrix and microwave spectroscopy (LR.-IR. and LR.-MW., respectively). Similar to the earlier study on ethylene ozonolysis the *cis*-2-butene experiments were mainly directed towards qualitative detection of a possibly complete set of minor but polyatomic products. Though in some earlier work [5] [6] complex products have been suggested on the basis of low resolution mass spectra and gas chromatography, unequivocal identification is lacking for a considerable number of species so far. Better insight into the gas-phase mechanism may possibly be gained if the complex minor products can be taken into account. Besides qualitative product analysis our work also aims at further investigation of the sensitivity and specificity of our novel experimental methods LR.-IR. and LR.-MW. As will be seen, earlier results of the product analysis of the *cis*-2-butene/ozone system will be considerably extended and substantiated by their aid.

2. Experimental. – 2.1. *Chemicals.* The 2-butene from *Messer-Griesheim* (purity 2.8) was used without further purification. – Ozone was prepared from pure oxygen (*Messer-Griesheim*, purity 4.8) by means of a *Fischer* ozonizer. For details see [14]. – For identification purposes secondary 2-butene ozonides were prepared by liquid-phase ozonolysis of *cis*-2-butene in butane at -78° . For isolation the solvent was pumped off and the gas phase surveyed by IR. spectroscopy. The pumping process was controlled in such a manner that formation of a solid residue was avoided at all times. The mixture of ozonides thus obtained was stored in gaseous state at room temperature. The compounds were identified by MS. [15], $^1\text{H-NMR}$. [16] and microwave spectroscopy [17], and the IR.-matrix and -gas-phase spectra were measured within 24 h. From the $^1\text{H-NMR}$, a ratio of the (eq,ax)- to the (eq,eq)-conformer of 54:46 was found in agreement with [17]. – Dry acetic anhydride was prepared from acetic anhydride and dicyclohexyl carbodiimide [18] and purified by a spinning-band-column distillation at 15 Torr. The purity was checked by GLC. – Acetic formic anhydride was prepared according to *Garven* by reacting water-free HCOOH with ketene [19], and purified by distillation at 10 Torr in a 75 cm spinning-band column. – The *cis*- and *trans*-2,3-epoxybutanes (IV) were prepared by the sequence



After acetylation of I by acetic anhydride and pyridine, the latter and acetic acid were removed by azeotropic distillation, and II was purified by fractional distillation. A mixture of II (0.6 mol) and 150 ml of aq. HCl-solution (36%) was saturated with gaseous HCl, sealed in an ampoule and stirred for 1 week at 30° . After neutralization with NaHCO_3 , the mixture was poured over ice, extracted with ether, and the ether removed to yield III which was directly used for III \rightarrow IV. Thus, crude III was added slowly to a solution of 60 g of KOH in 30 ml of H_2O at 90° , and the mixture IV distilled off. The latter was separated into the two stereoisomers by GLC. [20] and identified by on line GLC/IR.

2.2. *Instrumentation.* – 2.2.1. *Linear-reactor-infrared-matrix spectroscopy (LR.-IR.).* The set-up used for this technique has been described in the ethylene work [13]. The only change for the 2-butene study consisted in replacing the earlier reactor by a pyrex cylindrical reactor of 10 mm diameter and 100 mm length; it was equipped with an orifice consisting of a capillary steel tube of 70 mm length and 0.1 mm diameter. Reaction conditions used in the LR.-IR. study are collected in Table 1. In order to judge the influence of wall effects, the LR.-IR. experiments were complemented by experiments in an all glass (pyrex) spherical reactor of ca. 12 cm diameter equipped with two opposing capillary inlet tubes for the reactant/argon mixtures and an outlet capillary sampling the reaction mixture at distances of 1.5–3.7 cm in the symmetry plane perpendicular to the inlet tubes. Residence times in the reactor were estimated to be 15 to 70 s.

2.2.2. *IR.-matrix spectroscopy.* For the purpose of unequivocal identification of reaction products IR. spectra of a number of molecules isolated in Ar-matrices were taken. For preparation of the spectroscopic samples the molecules were deposited on a CsI window by means of a *Knudsen* cell, combined with a 4-nozzle system for the argon in a liq. He cryostat of our own design. M/A ratios in the range of 1000 to 5000 were chosen. Deposition rates were measured by means of a small

Table 1. Reactor conditions of LR.-IR. and LR.-MW. experiments

Experiment Type	Reactor No.	Reactor type	$p(\text{O}_3)$ [Torr]	$p(\text{cis-2-butene})$ [Torr]	$p(\text{Ar})$ [Torr]	τ_R^a [s]	Temp. [K]
IR.	1–3	Linear glass	30	30	690	48–75	298
IR.	4–5	Spherical glass	14	10	360	15–70	298
MW.	1–10	Linear glass	1–2	1–2	–	30	298
MW.	11–30	Linear stainless steel	1–2	1–2	–	30	298

a) τ_R = residence time.

He-Ne laser [21] and usually amounted to 3.0 $\mu\text{m}/\text{min}$. The matrix spectra were recorded on a *Perkin-Elmer* infrared photometer, model 325, with slit program 4 used primarily.

For the identification of primary ozonides matrix-reaction experiments were carried out in which the two Ar/reactant mixtures were deposited from separate nozzles at a distance of ca. 70 mm from the liq.-He-cooled CsI window. M/A-ratios of ca. 50 were used. After deposition the IR. spectrum was measured, and then the sample allowed to warm up to ca. 50 K within 70 min after which the cryostat was recooled to liq.-He-temp. During the warming-up the IR. was periodically scanned.

2.2.3. Linear-reactor-MW. spectroscopy. The LR.-MW. set-up has already been described [13]. In order to investigate wall effects two types of external linear reactors of a length of 100 cm and a diameter of 6.3 mm, made from stainless steel and pyrex, respectively, were used in this work. In all experiments both reactor and *Stark* cell were kept at room temperature. For enhancement of the sensitivity particular regions of the MW. spectra were scanned and digitally measured with a digital voltmeter under the control of a PDP-8/E computer. Usually, 30–150 scans were added and smoothed by quadratic polynomial interpolation.

An attempt was made to roughly estimate integrated absorption coefficients for some of the observed transitions of most of the complex reaction products and to derive from them particle concentrations. The integrated absorption coefficient is approximately given by

$$A_{mn} = (8\pi^3/3ckT) (N/Z) e^{-\frac{E_m}{kT}} \cdot \nu_{mn}^2 |\langle m|\hat{\mu}|n\rangle|^2$$

where ν_{mn} , E_m , $|\langle m|\hat{\mu}|n\rangle|^2$, N and Z denote transition frequency, energy eigenvalue of the lower state, transition moment (line strength factor), particle density and partition function, respectively [22]. For the purpose of this work the latter may be approximated by the usual factorization [23]

$$Z \approx Z_{\text{rot}} \cdot Z_{\text{vib}} \approx \frac{(8\pi)^{1/2} (kT)^{3/2} g^{1/2}}{\sigma h^3} \cdot \Pi (1 - e^{-(h/kT)\tilde{\nu}_m})^{-1},$$

and the energy eigenvalue E_m for a rotational transition $J''K''_u \leftrightarrow J'K'_u$ may be taken as

$$E_m = E_{J''K''_u} + \Sigma ch\tilde{\nu}_i \cdot \nu_i.$$

The statistical weight in the lower state reads (g_{ns} denotes the nuclear spin statistical weight)

$$g_m = (2J'' + 1) \cdot g''_{\text{ns}} \approx g_{\text{ns}}.$$

Since absolute intensity measurements with our present LR.-MW. system do not appear feasible, all intensity measurements were related to known lines of formaldehyde (integrated absorption coefficient A_{ij})

$$A_i = \frac{A_{mn}}{A_{ij}} = \frac{N}{N_a} \frac{(e^{-E_m/kT}/Z)}{(e^{-E_a/kT}/Z_a)} \cdot \frac{\nu_{mn}^2}{\nu_{ij}^2} \cdot \frac{|\langle m|\hat{\mu}|n\rangle|^2}{|\langle i|\hat{\mu}|j\rangle|^2}.$$

It is obvious that this approach involves considerable systematic and statistical errors arising from uncertainties of the baseline (overlapping *Stark* lobes, neighboring lines and spurious signals), variable operating conditions of the waveguide spectrometer, etc.

3. Results. - 3.1 LR.-IR. spectroscopy. A typical LR.-IR. spectrum as obtained under the conditions described in *Table 1*, i.e. reaction times of 48–75 s, is reproduced in *Figure 1*. The IR.-matrix spectra are qualitatively independent of the residence time (interval used 15–75 s, cf. *Table 1*) and the type of the reactor. *Figure 2* shows expanded sections of the LR.-IR. spectrum which are relevant for the identification of particular products. *Figure 3* encompasses IR.-matrix spectra of particular products which hitherto have not been published, these spectra were taken from the pure compounds and were required for identification purposes in LR.-IR. spectra.

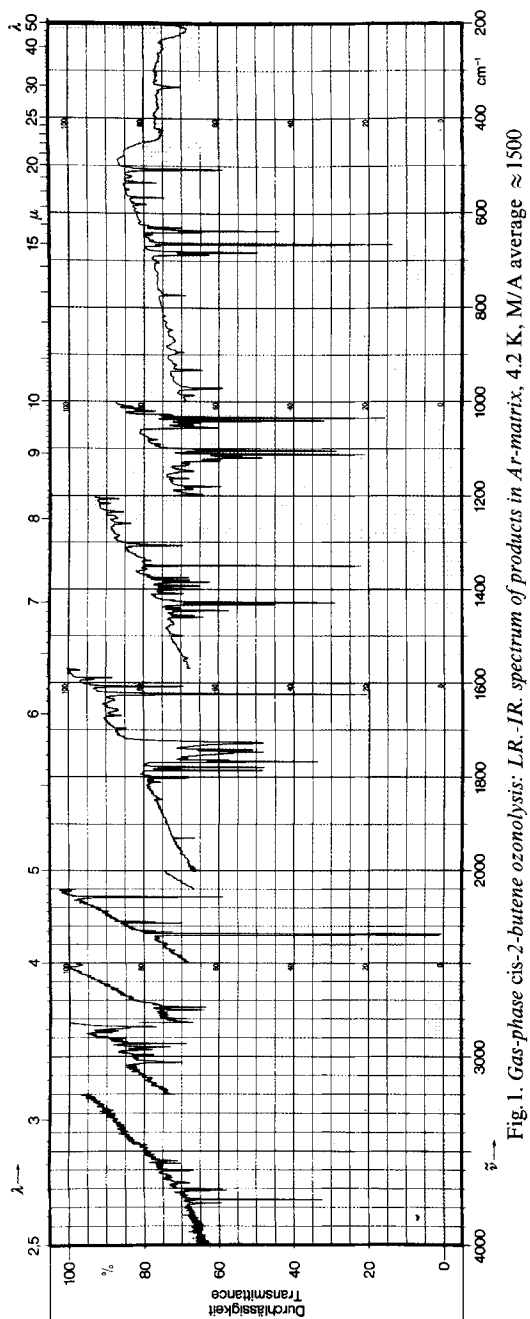


Fig. 1. Gas-phase cis-2-butene ozonolysis: L.R.-IR. spectrum of products in Ar-matrix, 4.2 K, M/A average ≈ 1500

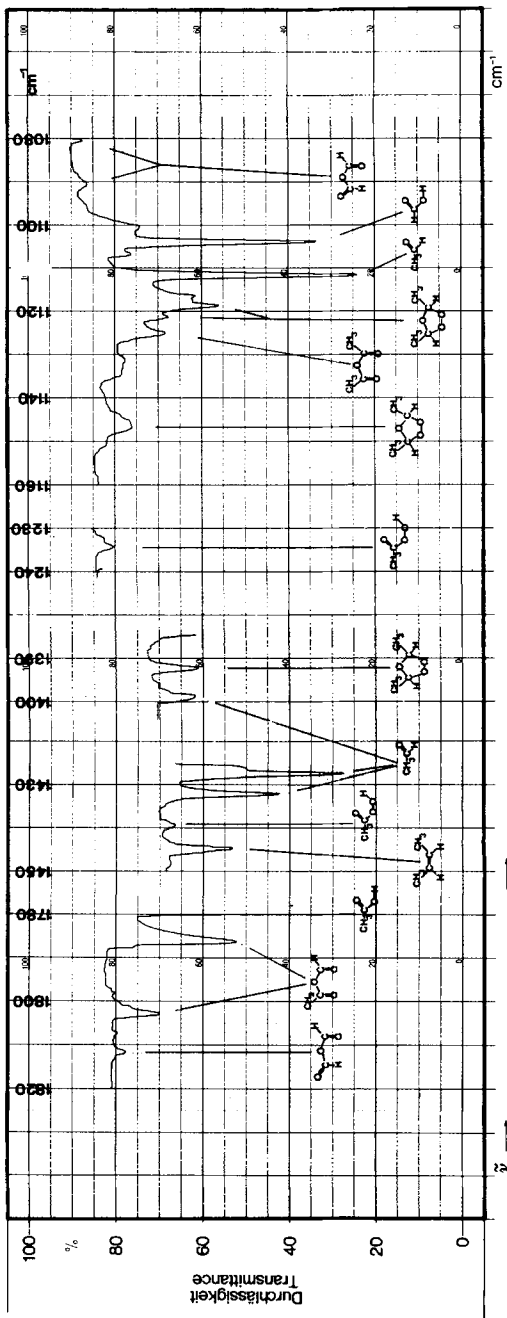


Fig. 2. Gas-phase cis-2-butene ozonolysis: expanded L.R.-IR. spectrum of products in Ar-matrix, 4.2 K, M/A average ≈ 1500

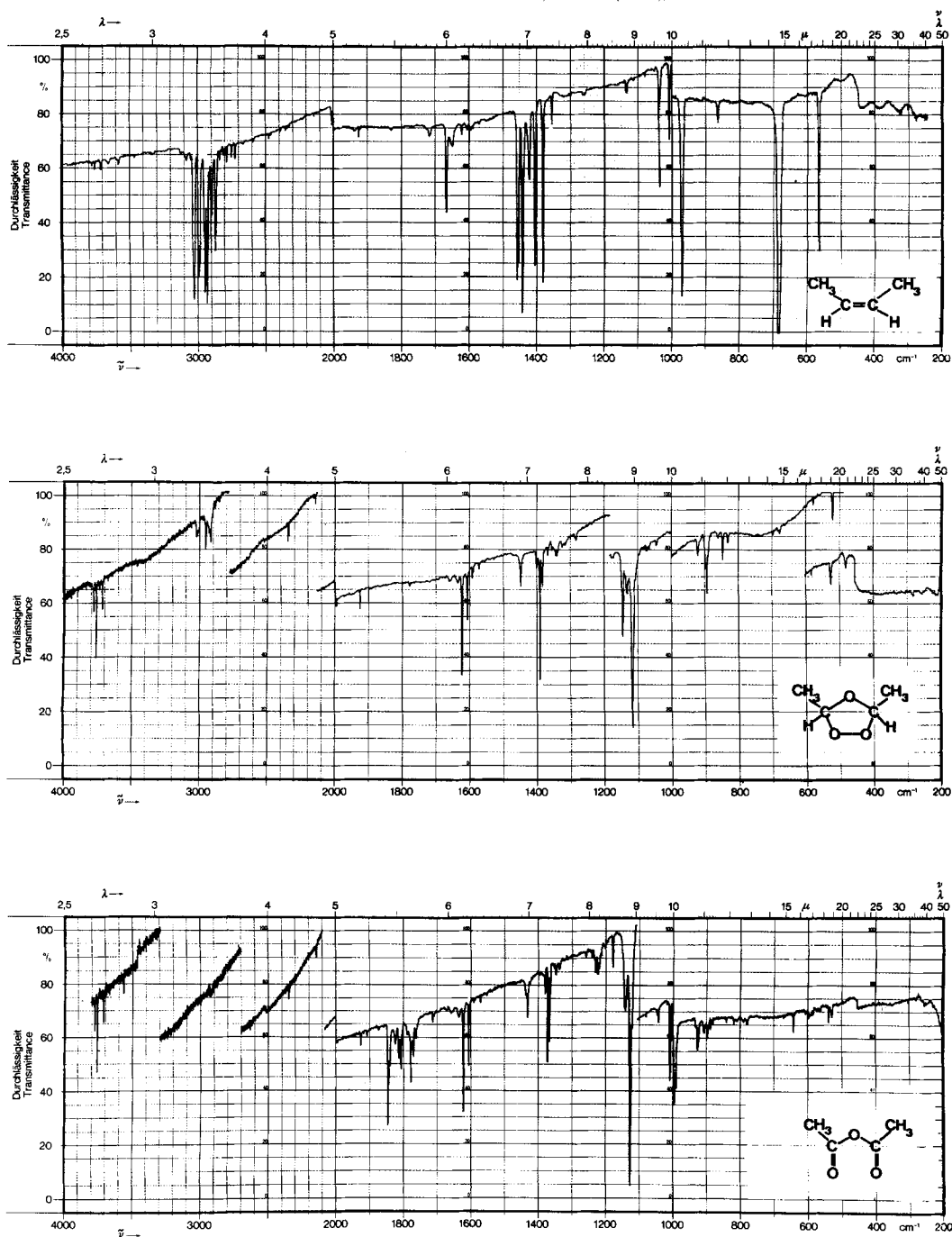
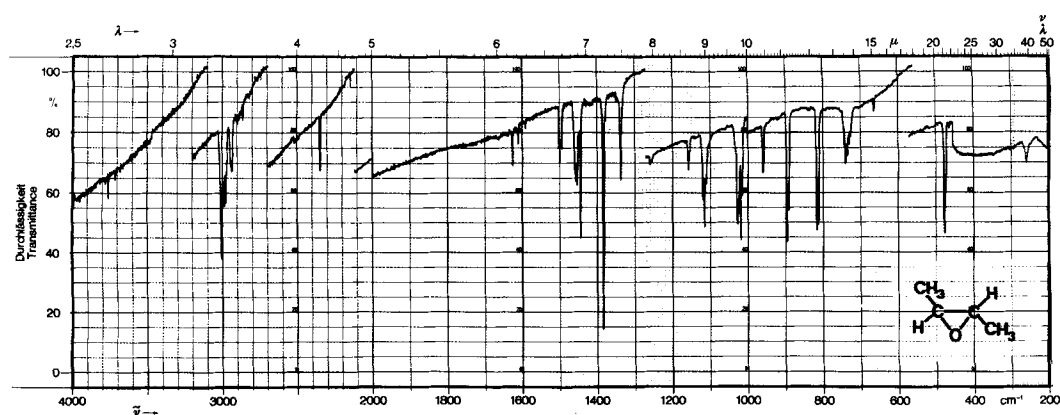
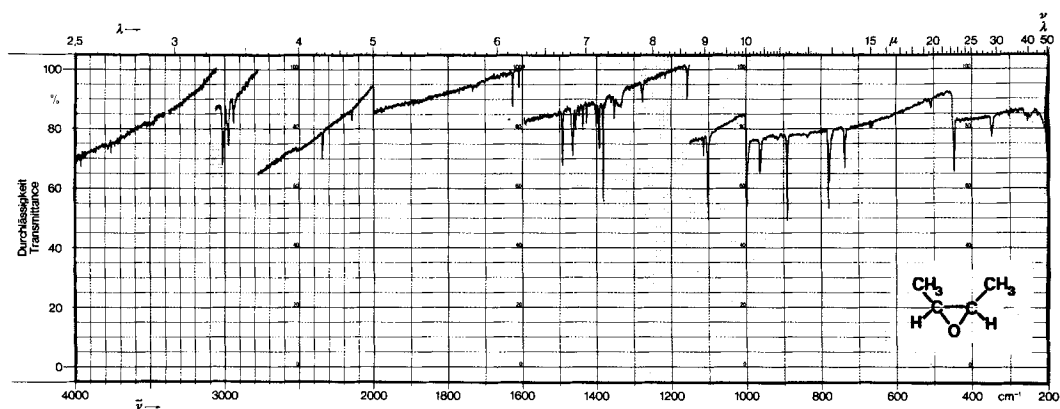
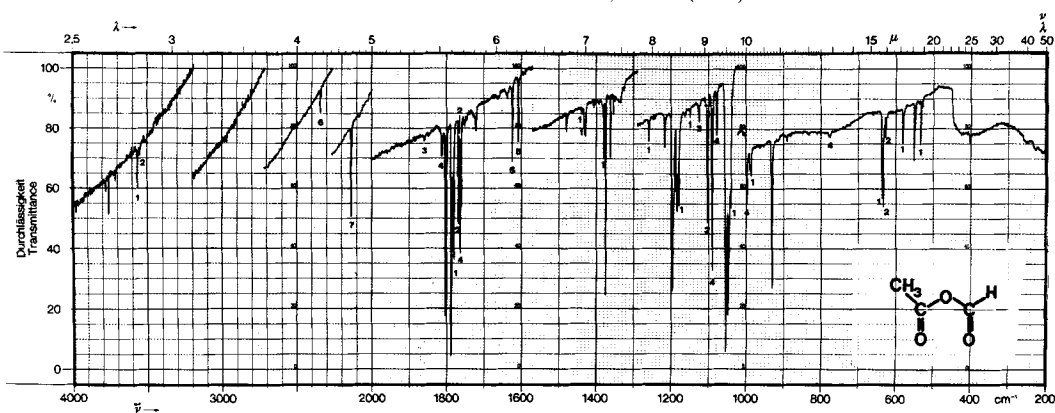


Fig.3. Reference IR. spectra of pure compounds in *Ar*-matrix, 4.2 K, M/A ratio for *cis*-2-butene 1000, for secondary ozonide of *cis*-2-butene (mixture of 2 stereoisomers) 1500, for acetic anhydride 2000, for acetic formic anhydride 4300, for *cis*-2-butene epoxide 2700, for *trans*-2-butene epoxide 1200. Acetic



formic anhydride contains impurities of acetic acid (1), formic acid (2), acetic anhydride (3), formic anhydride (4), water (5), CO₂ (6), and CO (7).

The rather complicated matrix spectrum of *trans*-2-butene epoxide is not due to a low M/A ratio. Increase of the latter to 5000 leaves the complicated matrix-band-shapes unaffected. The IR.-matrix spectrum of pure formic acetic anhydride could not be obtained since the samples always contained small amounts of acetic and formic acid, formic and acetic anhydride, and water. Lines corresponding to these species are numbered in *Figure 3*.

Table 2 gives a collection of key IR. matrix lines of the reference compounds used for identification of complex ozonolysis products. These matrix bands refer to the reference spectra shown in *Figure 3*.

Table 2. *cis*-2-Butene ozonolysis: list of identified products and typical spectral features (n.d. = not detectable)

Chemical species	IR. spectra (Ar matrix)		Reference compound		Microwave spectra	
	Ozonolysis mixture					
	Frequency [cm ⁻¹]	Intensity ^{a)}	Frequency [cm ⁻¹]	Intensity ^{a)}	Frequency [MHz]	Transition
O ₃	1040	<i>s</i>			23860	18 _{3,15} -19 _{2,18}
	1034	<i>vs</i> ^{b)}			25511	38 _{6,32} -30 _{5,35}
					25649	16 _{2,14} -17 _{1,17}
<i>cis</i> -2-butene	3029	<i>m</i>	3027	<i>vs</i>		
	2931	<i>m</i>	2929	<i>vs</i>		
	1445	<i>w</i>	1445	<i>vs</i>		
	970	<i>m</i>	971	<i>vs</i>		
	686	<i>m</i>	684	<i>vs</i>		
CO	2139	<i>s</i>				
¹² CO ₂	2350	<i>vs</i>				
	2342	<i>vs</i>				
	664	<i>vs</i>				
	663	<i>vs</i>				
¹³ CO ₂	2280	<i>m</i>				
	2274	<i>w</i>				
H ₂ O	3757	<i>s</i>			22235	6 _{1,6} -5 _{2,3}
	1624	<i>s</i>				
	1608	<i>m</i>				
CH ₂ O	2862	<i>w</i>	2862 ^{c)}	<i>s</i>	19595	25 _{4,21} -25 _{4,22}
	2799	<i>w</i>	2796	<i>s</i>	22966	9 _{2,7} - 9 _{2,8}
	1743	<i>m</i>	1742	<i>vs</i>	26559	26 _{4,22} -26 _{4,23}
	1498	<i>w</i>	1498	<i>s</i>		
	1167	<i>vw</i>	1167	<i>m</i>		
CH ₄ ^{d)}			3020	<i>w</i>		n.d.
	1306	<i>m</i>	1306	<i>s</i>		
HCOOH	3550	<i>w</i>	3551 ^{e)}	<i>m</i>	20293	11 _{2,9} -11 _{2,10}
	1768	<i>s</i>	1768	<i>vs</i>	22471	9 _{3,6} - 9 _{2,7}
			1115	<i>m</i>	24569	5 _{1,4} - 5 _{1,5}
	1104	<i>s</i>	1103	<i>vs</i>		
	636	<i>s</i>	636	<i>s</i>		
CH ₃ OH	3669	<i>vw</i>	3667 ^{f)}	<i>m</i>	19967	2,1- 3,0E(-)
	2955	<i>w</i>	2956	<i>m</i>	25018	6,2- 6,1E(-)
	2847	<i>w</i>	2848	<i>m</i>	25125	7,2- 7,1E(-)
	1034	<i>vs</i>	1034	<i>vs</i>	25878	10,2- 10,1E(-)
	1027	<i>w</i>	1028	<i>s</i>		

Table 2 (continued)



Chemical species	IR. spectra (Ar matrix)					
	Ozonolysis mixture		Reference compound		Microwave spectra	
	Frequency [cm ⁻¹]	Intensity ^{a)}	Frequency [cm ⁻¹]	Intensity ^{a)}	Frequency [MHz]	Transition
(HCO) ₂ O	1812	<i>vw</i>	1812 ^{g)}	<i>m</i>	n.d.	
	1761	<i>vw</i>	1762	<i>s</i>		
	1090	<i>vw</i>	1090	<i>s</i>		
	1081	<i>vw</i>	1079	<i>m</i>		
	–	–	227	<i>m</i>		
CH ₃ CHO	1728	<i>s</i>	1727 ^{h)}	<i>s</i>	19226	1 _{0,1} -0 _{0,0} 1A
	1432	<i>s</i>	1432	<i>vs</i>	19262	1 _{0,1} -0 _{0,0} 0E
	1428	<i>s</i>	1427	<i>vs</i>	19265	1 _{0,1} -0 _{0,0} 0A
	1349	<i>vs</i>	1349	<i>vs</i>	19268	1 _{0,1} -0 _{0,0} 1E
	1112	<i>vs</i>	1111	<i>vs</i>		
CH ₃ COOH	3564	<i>w</i>	3566 ⁱ⁾	<i>w</i>	20209	8 _{5,4} -8 _{5,3}
	1780	<i>s</i>	1779	<i>vs</i>	24588	8 _{5,3} -8 _{6,2}
	1259	<i>w</i>	1259	<i>m</i>	50249	9 _{5,4} -9 _{6,3}
	1180	<i>m</i>	1181	<i>vs</i>		
	639	<i>m</i>	639	<i>s</i>		
CH ₂ (OH)CHO		n.d.			22143	4 _{0,4} - 4 _{1,3}
					24367	{ 24 _{13,12} -25 _{12,13}
					40245	{ 24 _{13,11} -25 _{12,13}
						12 _{6,7} - 11 _{7,4}
CH ₃ CO ₃ H	1439	<i>w</i>	1439 ^{k)}	<i>s</i>	21688	3 _{0,3} -2 _{0,2} A
	1234	<i>w</i>	1234	<i>s</i>	20398	3 _{1,3} -2 _{1,2} A
	618	<i>vw</i>	619	<i>m</i>	22650	3 _{0,3} -2 _{0,2} E
	422	<i>vw</i>	422	<i>s</i>		
	319	<i>vw</i>	319	<i>m</i>		
					19455	5 _{1,5} -4 _{1,4} E
CH ₃ COOCHO	1803	<i>m</i>	1803 ^{l)}	<i>vs</i>	21439	5 _{1,4} -4 _{1,3} E
	1786	<i>s</i>	1787	<i>vs</i>	24101	6 _{0,6} -5 _{0,5} E
	1375	<i>m</i>	1375	<i>s</i>	24103	6 _{0,6} -5 _{0,5} A
	1196	<i>w</i>	1197	<i>s</i>	25679	6 _{1,5} -5 _{1,4} A
	1055	<i>m</i>	1057	<i>vs</i>	25684	6 _{1,5} -5 _{1,4} E
(CH ₃) ₂ C=C=O		n.d.			18936	40 _{13,27} -40 _{13,28}
					19856	37 _{12,25} -37 _{12,26}
					21801	28 _{9,19} -28 _{9,20}
					22033	25 _{8,17} -25 _{8,18}
					25701	47 _{15,32} -47 _{15,33}
<i>cis</i> 						
CH ₃ CHCHCH ₃		n.d.	1383	<i>s</i>	20201	11 _{3,8} - 11 _{4,7}
			1103	<i>s</i>	23798	8 _{3,5} - 8 _{3,4}
			998	<i>s</i>	26073	16 _{5,11} -16 _{6,11}
			891	<i>s</i>		
			781	<i>s</i>		
<i>trans</i> 						
CH ₃ CHCHCH ₃		n.d.	3007	<i>s</i>	22524	10 _{2,8} - 10 _{1,9}
			1385	<i>vs</i>	22693	11 _{2,9} - 11 _{1,10}

Table 2 (continued)

Chemical species	IR. spectra (Ar matrix)					
	Ozonolysis mixture		Reference compound		Microwave spectra	
	Frequency [cm ⁻¹]	Intensity ^{a)}	Frequency [cm ⁻¹]	Intensity ^{a)}	Frequency [MHz]	Transition
CH ₃ COCH ₂ CH ₃			1383	vs	23180	12 _{2,10} -12 _{1,11}
			896	s	24022	12 _{2,11} -13 _{1,12}
			473	s	24337	16 _{4,12} -15 _{5,11}
		n.d.			18849	6 _{1,5} -6 _{0,6} E
					19085	8 _{2,6} -8 _{1,7} E
(CH ₃ CO) ₂ O					19190	8 _{2,6} -8 _{1,7} A
					23639	7 _{1,6} -7 _{0,7} E
	1847	vw	1848	s	n.d.	
	1845	vw	1845	w		
	1369	vw	1368 ^{m)}			
Secondary ozonide of 2-butene	1125	w	1126	vs		
	1006	vw	1008 ^{m)}	s		
	1393	m	1393	s	20567	16 _{3,13} -16 _{2,14}
	1147	w	1147	s	23168	17 _{3,14} -17 _{2,15}
	1119	m	1119	vs	23358	20 _{4,16} -20 _{3,12}
	893	w	894	s	25441	22 _{5,17} -22 _{4,18}
	522	vw	522	m		

^{a)} vw very weak, w weak, m medium, s strong, vs very strong. ^{b)} O₃ together with CH₃OH, 1033 cm⁻¹ (O₃). ^{c)} P. Felder, private communication. ^{d)} M. Dubs, private communication. ^{e)} [24]. ^{f)} [25]. ^{g)} [26]. ^{h)} [27]. ⁱ⁾ [28]. ^{k)} [29]. ^{l)} [30]. ^{m)} Site multiplets.

3.1.1. *IR. spectra of matrix reaction species.* Figure 4 presents the IR. matrix spectra of equimolar amounts of O₃ and *cis*-2-butene. The four expanded reaction spectra B were taken during the warming up experiment, and the spectrum C having recooled to liquid He temperature (s. exper. part). The frequency range of the expanded sections was chosen in order to show bands which may be characteristic for the primary ozonide (poz) [4].

3.2. *LR.-MW. spectroscopy.* Relevant results of LR.-MW. spectroscopy of the *cis*-2-butene ozonolysis are collected in Table 2 as obtained from experiments carried out under conditions listed in Table 1. In Table 2 only a few of the MW. transitions used to identify particular products were retained. As a rule for positive identification of products 3–5 rotational transitions were considered to be sufficient. The application of signal averaging for detection of weak MW. absorption lines somewhat hindered the observation of the transient behavior of particular products. In this work no detailed information about switch-on/switch-off experiments is given though for some of the species aspects of this type are mentioned in connection with the mechanistic scheme of the ozonolysis.

Relative particle concentrations as estimated by the procedure described in chap. 2.2.3 are collected in Table 3. It should be remembered that these values indicate only orders of magnitude. The errors inherent to the estimates also involve approximations made for calculation of the sum of states (rigid-rotor-harmonic-oscillator approximation, internal rotation considered as harmonic oscillators, etc.).

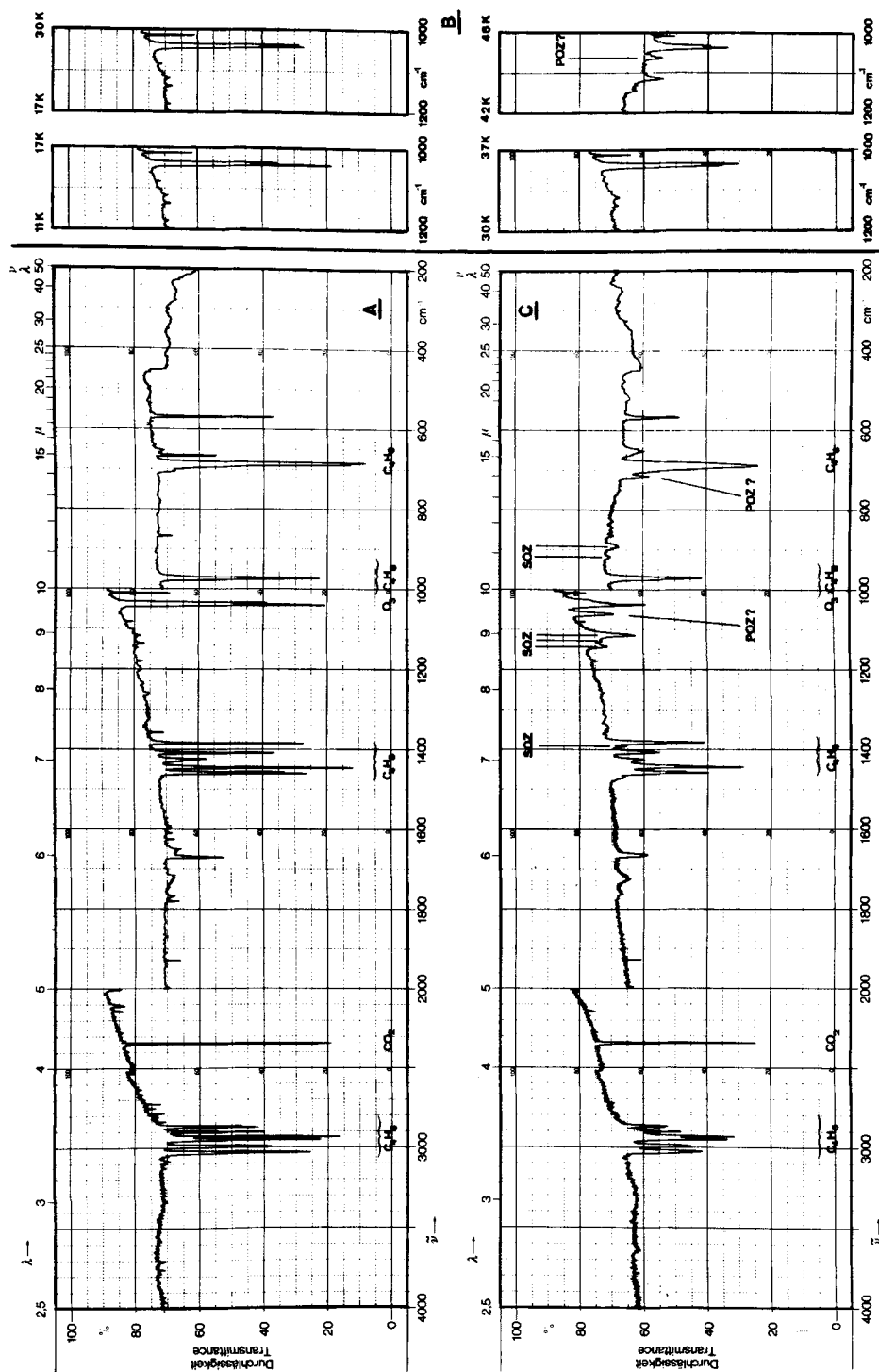


Fig. 4. *cis*-2-Butene ozonolysis in Ar-matrix, IR spectra. A) of reactants at 4.2 K, B) during warm-up, and C) after recooling to 4.2 K. M/A \approx 50. POZ = primary ozonide, SOZ = secondary ozonide

Table 3. LR.-MW. of *cis*-2-butene ozonolysis: approximate relative concentrations of complex products

Product	Relative concentration	Particle density ^{a)} [cm ⁻³]	Ref.
H ₂ CO	1		[31]
HCOOH	3-5 · 10 ⁻³		[24] [32]
CH ₃ OH ^{b)} c)	2-3 · 10 ⁻²		[33]
CH ₃ CHO	0.2-0.3 ^{a)}	5-8 · 10 ¹⁵	[34] [35]
(HCO) ₂ O	n.d. ^{d)}		-
CH ₃ COOH	3-5 · 10 ⁻³		[36] [37]
CH ₃ CO ₂ H	1-2 · 10 ⁻⁴		[29] [38]
CH ₂ (OH)CHO ^{e)}	1-2 · 10 ⁻⁴		[39]
CH ₃ COOCHO	n.d. ^{d)}		-
(CH ₃) ₂ C=C=O	3-6 · 10 ⁻⁴		[40]
CH ₃ COCH ₂ CH ₃	n.m. ^{f)}		-
<i>cis</i> -CH ₃ CHCH(O)CH ₃ ^{e)}	4-12 · 10 ⁻⁵	1-3 · 10 ¹²	[41]
<i>trans</i> -CH ₃ CHCH(O)CH ₃ ^{e)}	2-6 · 10 ⁻⁵	0.5-1.5 · 10 ¹²	[42]
(CH ₃ CO) ₂ O	n.d. ^{d)}		-
(eq.eq)-CH ₃ O—O CHOCHCH ₃ ^{e)}	2-4 · 10 ⁻³		[43]

a) For experiments with $p_R \approx 2-4$ Torr, total pressure in waveguide: 80 mTorr, partial pressure of CH₃CHO: 4(2) mTorr.

b) Fundamental modes estimated.

c) By direct calibration.

d) Not detectable in LR.-MW. experiments.

e) Electric dipole moment estimated.

f) Not measurable due to overlapping lines.

4. Discussion. - The experimental results presented above will be discussed from various points of view: survey of data, including characteristic features of LR.-IR. and LR.-MW. experiments, wall effects and discrepancies, conceivable mechanisms of complex product formation, possible influence of radical reactions and comparison with other work.

4.1. *Discussion of the experimental results.* - 4.1.1. *Comparison of characteristic features of LR.-IR. and LR.-MW. experiments, and consequences for the behavior of radicals.* Since by the two experimental techniques used in this work the same reaction is followed under widely different pressure conditions, it appears worthwhile to contrast the most important characteristic parameters defining mechanism and kinetics of the process. LR.-IR. experiments were carried out at total pressures of 600 Torr with foreign gas pressure 20-50 times higher than reactant partial pressures. In LR.-MW. experiments total pressures in the order of magnitude of 1 Torr were applied and no third body gas was admitted. Further comparison between the two experimental techniques is afforded by Table 4 where physical characteristics of the reactor experiments like dimensions (L_r , d_r), volume (V_r), surface (A_r), average flow velocity (\bar{v}), residence time (τ_r), typical diffusion coefficients (D) and typical decay length (l_e^{-1}) for radicals by wall reactions are collected. The latter are calculated from the expression [44]

$$[R](z) \approx [R](0) \exp(-3.671 \cdot z \cdot D / \bar{v}r^2).$$

which describes the decay of the concentration $[R]$ of the radical R along the axis of a linear reactor if every wall collision destroys the radical (z =axial distance from the radical source, r =reactor radius). Diffusion coefficients were estimated by the *Stefan-Maxwell* approximation [45]

$$D \approx (3 \pi \sigma^2 (N_1 + N_2))^{-1} (8 kT / \pi \mu)^{1/2}$$

for the radical V (s. *Scheme 1*, below) in Argon or in O_3 , with the collision parameter σ estimated from *Van der Waals* atomic radii [46]. The most important feature emerging from *Table 4* is the fact that in both types of experiments radicals subject to destruction by wall collisions would be rather efficiently removed from the homogeneous gas reaction, since in both cases t_c^{-1} is $< 10^{-2}$ cm for complex radicals of the type V . This probably applies also to small radicals like O_2H , CHO and others which have been considered in the ozonolysis mechanism [5] [6] [9] [10] [47-49]. Therefore, it appears adequate to admit as few radical reactions as possible for the formation of the complex products observed in this work. Nevertheless, radicals may still be involved in these processes as intermediates in homogeneous reactions (see chap. 4.3.2).

The two types of experiments with respect to the specific collision frequency factor

$$Z_{AM} \approx \pi \sigma_{AM}^2 (8 kT / \pi \mu_{AM})^{1/2}$$

but differ by orders of magnitude with respect to the collision deactivation rate constant [50] [51]

$$k_{\text{deact}} \approx Z_{AM} \cdot N_M.$$

Table 4. *Typical characteristic features of reactor experiments*

Quantity ^{a)}	LR.-IR.	LR.-MW.
d_r (cm)	1.0	0.63
L_r (cm)	{ 10.0 12 (sphere)	100
V_r (cm ³)	{ 8 905 (sphere)	31
A_r (cm ²)	{ 30 450 (sphere)	200
p_{total} (Torr)	600	2
ϕ_r (cm ³ s ⁻¹) ^{b)}	{ 0.16-0.11 19-12 sphere	1
\bar{v} (cms ⁻¹) ^{c)}	0.20-0.13	3.2
τ_r (s) ^{d)}	48-75	30
D (cm ² s ⁻¹) ^{e)}	0.2	50
t_c^{-1} (cm) ^{f)}	$7 \cdot 10^{-3}$	$1.7 \cdot 10^{-3}$
Z_{AM} (cm ³ s ⁻¹) ^{g)}	$2.5-3 \cdot 10^{-10}$	$2.5-5 \cdot 10^{-10}$
k_{deact} (s ⁻¹) ^{h)}	$4.5 \cdot 10^9$	$0.8-1.6 \cdot 10^7$

a) For notation cf. chap.4.1.1.

b) Volume flow in the reactor.

c) Average gas flow velocity.

d) Residence time.

e) Diffusion coefficient for typical radical V (s. *Scheme 1*).

f) Compare equation in 4.1.1.

g) Specific collision frequency factor.

h) Collision deactivation rate constant.

Since many particular steps of the ozonolysis mechanism are highly exothermal, decomposition of non-thermalized products into radical fragments should be suppressed more efficiently under LR.-IR. conditions.

4.1.1.1. *Wall effects.* Wall effects may play a role in LR.-IR. and LR.-MW. experiments by eliminating radicals from the gas phase and by heterogeneous catalysis of relevant reactions. From the above mentioned estimations one would argue that radical scavenging by reactor walls will be of importance. Heterogeneous catalysis, however, appears much less effective since neither the material nor the widely varying surface-to-volume ratio of the reactor (0.5 to 6 cm^{-1} , cf. Table 4) seems to play an obvious role in the yields of complex ozonolysis products. The latter all show, in the case of *cis*-2-butene, essentially the same appearance kinetics including the secondary ozonide. This again indicates wall effects are not dominant under the conditions of this work.

It should be mentioned that wall effects of similar kind and magnitude as discussed above, have to be anticipated for work based on other techniques. This may be concluded from consideration of typical experimental conditions reported by various workers [9] [10] [47].

4.1.2. *Comparison of the product analysis obtained by LR.-IR. and LR.-MW., respectively.* Typical results found by both LR.-IR. and LR.-MW. may be commented upon as follows: (i) In a broad sense the set of products from *cis*-2-butene ozonolysis is closely analogous to that from ethylene ozonolysis [13], though *cis*-2-butene yielded a larger diversity of complex products. This is made obvious by the following comparison in which only complex products are listed:

Ethylene ozonolysis	<i>cis</i> -2-Butene ozonolysis
–	CH_4
CH_3OH	CH_3OH
$\text{H}_2\text{CO}, \text{CH}_3\text{CHO}$	$\text{H}_2\text{CO}, \text{CH}_3\text{CHO}, \text{CH}_3\text{COCH}_2\text{CH}_3$
$\text{CH}_2\text{CH}_2\text{O}$	<i>cis</i> - and <i>trans</i> - $\text{CH}_3\text{CHCH}(\text{O})\text{CH}_3$
HCOOH	$\text{HCOOH}, \text{CH}_3\text{COOH}, \text{CH}_3\text{CO}_3\text{H}$
$\text{CH}_2(\text{OH})\text{CHO}$	$\text{CH}_2(\text{OH})\text{CHO}$
$(\text{HCO})_2\text{O}$	$(\text{HCO})_2\text{O}, \text{HCOOCOCH}_3, (\text{CH}_3\text{CO})_2\text{O}$
	$(\text{CH}_3)_2\text{C}=\text{C}=\text{O}$
	Secondary ozonide

(ii) Both experimental techniques yield similar results with respect to identified products. Table 2 demonstrates clearly the high ability of LR.-IR. and LR.-MW. for unequivocal identification of complex products at low concentration levels. It also shows that the two techniques complement each other in a favorable way, particularly for detection of species with low electric dipole moment or with numerous low lying vibrational modes.

(iii) Discrepancies in the results obtained from LR.-IR. and LR.-MW. may be traced back to differences in sensitivity for particular species [13] and for differences in the extent of reaction owing to widely different pressure range and the concentration of foreign gas, cf. Tables 1 and 4. A few typical examples may

illustrate such discrepancies. Acetic anhydride is definitely detectable by LR.-IR. but has not been found in LR.-MW. experiments. However, the MW. spectrum of acetic anhydride has not been observed so far due to weak absorption lines [30]. Formic anhydride may be considered as a limiting case since it has been identified by 5 very weak key bands in the IR. but escaped detection in LR.-MW. experiments. On the other hand, 2,3-epoxybutanes have not been detectable by LR.-IR. though both stereoisomers (*cis* and *trans*) are unambiguously identified by LR.-MW. This discrepancy is probably due to higher sensitivity of the latter method. Finally, an extreme example is given by CH_4 , which naturally is detectable only by LR.-IR.

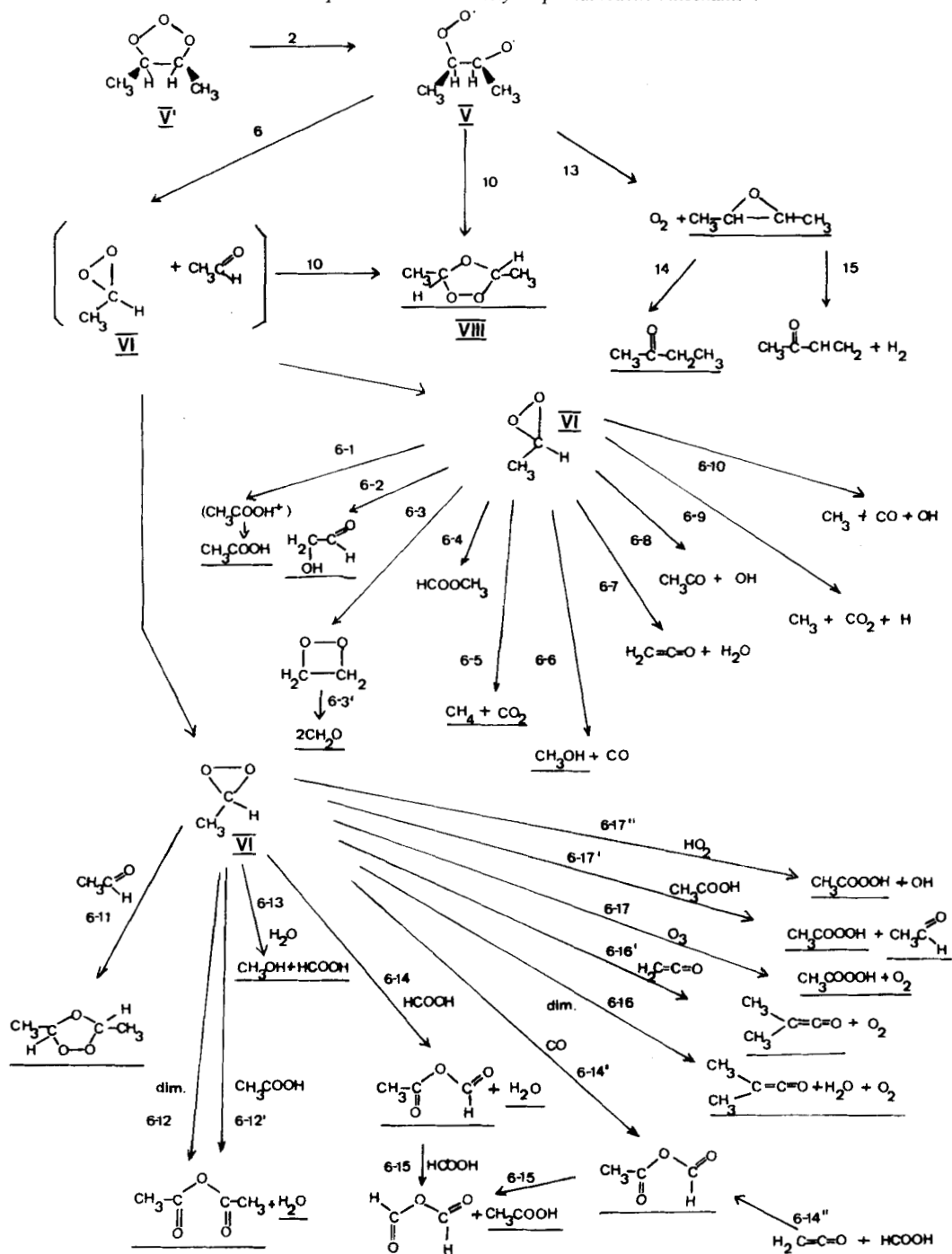
4.1.3. *Specific LR.-MW. results.* A few of the LR.-MW. results deserve specific comments: (i) In contrast to LR.-IR. the LR.-MW. method permits qualitative observation of transient behavior of reaction products in switch on/off experiments. From such experiments, which correspond to started/stopped-flow experiments, information about kinetic constants is in principle derivable. However, adsorption phenomena and the flow dynamics of the waveguide cell render quantitative analysis of transient experiments rather difficult.

Qualitatively it was found that the transient kinetics of the secondary ozonide of 2-butene is essentially the same as that of other ozonolysis products. This should be contrasted with the findings in the ethylene ozonolysis, where the secondary ozonide was not observed in LR.-MW. experiments carried out at room temperature. Only in ethylene-ozonolysis experiments at -60° the ozonide was detectable, but after retardation times of the order of hours. Therefore, the appearance of the secondary ethylene ozonide was attributed to wall reactions. In view of this the secondary 2-butene ozonide may be considered as a product of the homogeneous gas-phase ozonolysis of *cis*-2-butene. So far the LR.-MW. experiments allowed only the identification of the (eq,eq)-conformer of the secondary ozonide. The MW. spectra of other conformers cannot be identified at the present time, and thus their formation remains an open question.

(ii) LR.-MW. allows unique identification of *cis*- and *trans*-2,3-epoxybutane (cf. Table 2). This fact appears to have significant implications for the mechanism of the ozonolysis, as will be discussed below.

4.1.4. *Comparison to earlier work on product analysis.* With regard to the following discussion it appears appropriate to briefly compare the set of products identified unequivocally in this paper with those reported in preceding work. By far the most extended set of products for *cis*-2-butene ozonolysis has been reported by Atkinson *et al.* [5] and by Finlayson *et al.* [6] (s. chap. 1). Among the complex products reported H_2O_2 , $\text{CH}_2=\text{C}=\text{O}$, $(\text{CHO})_2$ and $\text{CH}_2=\text{CHCOCH}_3$ have not been found in our work in spite of specific efforts directed toward their detection. However, it should be pointed out that they were observed mostly in presence of excess O_2 [5] [6]. The formation of 2-butanone and 3-buten-2-one is usually explained as resulting from addition and abstraction reactions of *cis*-2-butene with OH radicals. Since the reaction conditions in the work cited above closely parallels those of our LR.-MW. experiments, it appears necessary to retain the possibility of radical reactions also for LR.-IR. and LR.-MW. experiments besides those considered in the Scheme discussed below.

Scheme 1. Gas-phase 2-butene ozonolysis: partial reaction mechanism



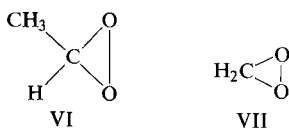
4.2. Ozonolysis in argon matrix; indication for the presence of the primary ozonide.

As documented by *Figure 4*, a set of new bands appear during the warm-up period from liquid He temperature. With the exception of the two bands near 1062 and 715 cm^{-1} they can all be assigned to the secondary ozonide. Although for the highly concentrated matrix ($M/A \approx 50$) noticeable matrix shifts are to be expected with respect to high M/A spectra, the secondary ozonide bands exhibit in fact quite small shifts in the majority of cases ($< 0.5 \text{ cm}^{-1}$). Therefore one might state that secondary ozonide formation in the Ar-matrix occurs in the temperature range $< 50 \text{ K}$.

The two bands at 1062 and 715 cm^{-1} have not been observed in any other spectra known to us. Their location closely corresponds to bands at 1050 and 710 cm^{-1} reported by *Heicklen et al.* [4] which were assigned, together with a set of further bands, to a primary ozonide. However, the latter set of bands clearly coincides with secondary ozonide bands. Although the two extra bands appear to indicate formation of a new molecular species, they do not afford a sufficient basis for the identification of a primary ozonide. *Heicklen's* interpretation therefore seems untenable.

4.3. *Conceivable mechanism of complex product formation.* Based on the detection of the complex products referred to above, one may attempt to formulate a partial reaction mechanism of the *cis*-2-butene ozonolysis (s. *Scheme 1*). This mechanism consists of two main routes²⁾: (i) decomposition reactions of the primary ozonide V' or biradical V in which the two C-atoms of the *cis*-2-butene C,C double bond remain connected (epoxide formation), and (ii) decomposition of $V(V')$ into methyldioxirane (VI) or the *Criegee* intermediate (zwitter ion) and acetaldehyde and subsequent reactions of these.

The first few steps up to the formation of the biradical V and the *Criegee* intermediates are taken over from the general scheme proposed by *O'Neal & Blumstein* [7]. Most of the complex products can be explained by the intermediate



formation of methyldioxirane (VI) and a variety of reactions of VI – rearrangement, decomposition and dimerization reactions. A similar scheme has been taken into consideration for 2-butene ozonolysis by *Hansen et al.* [47], for propene and 2-methyl-1-propene by *Herron & Huie* [10] and for ethylene by *Herron & Huie* [9]. In the latter case the existence of dioxirane (VII) has been proven directly by MW. spectroscopy by *Lovas & Suenram* [52] and confirmed by low resolution mass spectroscopy by *Martinez et al.* [53]. However, as pointed out in chap. 1, the experimental data on complex products available from the study [9] [10] has been considerably narrower and less unambiguous.

The thermokinetic aspects of the formation and decomposition of the primary

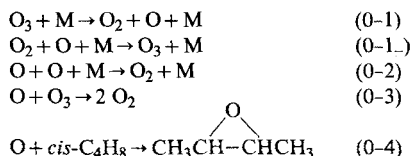
²⁾ Numbering of the reactions in *Scheme 1* is chosen in accord with the numbering used in the previously published reaction scheme for ethylene ozonolysis [13].

ozonide V' and biradical V have been discussed by *Benson* for the ethylene case [54] and apply with straightforward modification here.

In the following sections some of the more relevant aspects of the mechanism will be discussed.

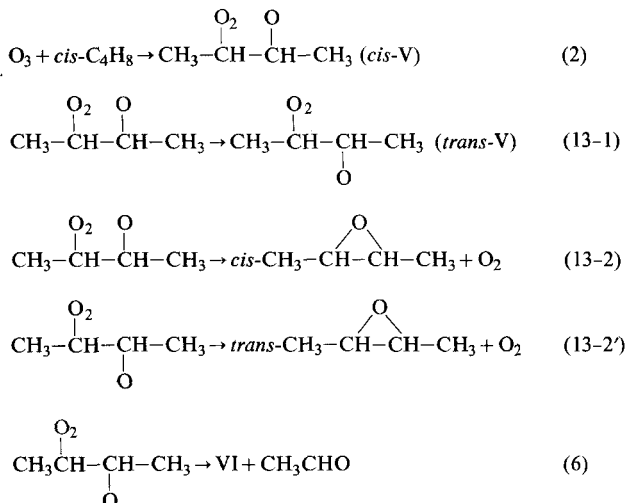
4.3.1. *Interpretation of 2,3-epoxybutane formation.* The unequivocal observation of both *cis*- and *trans*-2,3-epoxybutane offers some indication for the existence of the biradical intermediate V. This may be seen as follows. Direct formation of epoxides from olefins and O(³P) is known to be non-stereospecific [55]. Stereospecificity of the addition of O₃ to olefins in the gaseous phase apparently has not been investigated. However, for liquid phase ozonolysis it is commonly assumed that *cis*-addition occurs to olefins with non-terminal double bond [12].

Scheme 2



O-Atoms might be produced by other reactions in the ozonolysis process (see below).

Scheme 3



Taking the conditions used in this work one may assume the production of the two stereoisomeric 2,3-epoxybutanes to result from the reactions (2) and (13) (*cf.* Scheme 1). This amounts to consider the kinetic system given in Schemes 2 and 3. For reactions (0-1) to (0-4) in Scheme 2 the rate constants are known [56] or can be estimated; for processes in Scheme 3 some assumptions have to be made. The rate data used are collected in Table 5 and should be commented upon as follows: (i) For production of the biradical V the rate constant reported for the O₃ consumption by *cis*-2-butene may be considered representative [6] [56].

Table 5. Reaction rate constants for 2,3-epoxybutane formation

Reaction no. ^{a)}	Rate constant ^{b)}	Ref.
0-1	$1.0 \cdot 10^{-26}$	[56]
0-1 _{...}	$4 \cdot 10^{-34}$	[56]
0-2	$5 \cdot 10^{-33}$	[56]
0-3	$1.5 \cdot 10^{-14}$	[56]
0-4	$1.5 \cdot 10^{-11}$	[56]
2	$1.5 \cdot 10^{-16}$	[56]
13-1	$8 \cdot 10^{10}$	[57]
13-2,2'	$10^{-5}-10^5$	[this work]

^{a)} S. Schemes 1-3.

^{b)} First order rate constants in s^{-1} , 2nd order in $(\text{molec. cm}^{-3})^{-1} s^{-1}$, and 3rd order in $(\text{molec. cm}^{-3})^{-2} s^{-1}$.

(ii) The rate constant for the transformation of the *cis*-conformer of the biradical V into its *trans*-conformer may be estimated from [57]

$$k_{13-1} \approx 2 \nu_T \exp \{ -V/RT \}$$

where $\nu_T (\approx 150 \text{ cm}^{-1})$ and $V (\approx 1000 \text{ cm}^{-1})$ stand for the frequency of the C-C torsional mode and for its barrier to internal rotation. This leads to the value in Table 5, which obviously is very high. In fact, it practically amounts to the assumption that the reactions (2)-(13-1)-(13-2)-(13-2') produce both isomers at the same rate.

(iii) There is little kinetic data available which might serve as examples for the biradical decomposition reactions (13-2). Widely varying estimates for the *A*-factor (10^{10} to 10^{15} s^{-1}) and activation energy for the decay reaction of thermalized V ($30_{-10}^{+30} \text{ kcal/mol}$) suggest the calculation of integral curves of the kinetic system given in Schemes 2 and 3 for a wide range of values of $k_{13-2} = 10^{-15}$ to 10^{10} s^{-1} .

(iv) Inclusion of reaction (6) may serve to derive a more realistic limit for epoxide production since it competes with processes (13-2) and (13-2').

Extended numerical calculations of integrals of the kinetics equations associated with Schemes 2 and 3 have been carried out both with and without inclusion of step (6). The results of this kinetic modelling may be stated as follows.

The ratio

$$R(100 \text{ s}) = \frac{\text{epoxide concentration produced by reactions (0)}}{\text{epoxide concentration produced by reactions (13)'}}$$

evaluated at $t=100 \text{ s}$ as a function of k_{13-2} keeping all other rate constants at the values given in Table 5, is shown in Figure 5. It demonstrates that epoxide production mainly stems from reactions (0-1) to (0-4) if $k_{13-2} < 10^{-10} \text{ s}^{-1}$ and predominantly from biradical V if $k_{13-2} > 10^{-6} \text{ s}^{-1}$. Inclusion of reaction (6) with $k_6 = 0.1 \cdot k_{13-2}$ to $10 \cdot k_{13-2}$ does not alter this result noticeably.

Epoxide production from $O(^3P)$ addition to the olefin would never, within the frame set by the rate constants collected in Table 5, produce the epoxides with higher particle density than 10^9 cm^{-3} after 100 s under the conditions of our experiments. In order to achieve epoxide concentrations of the order of magnitude observed in this work, i.e. $1-4 \cdot 10^{12} \text{ cm}^{-3}$, cf. Table 3, production *via* the reaction

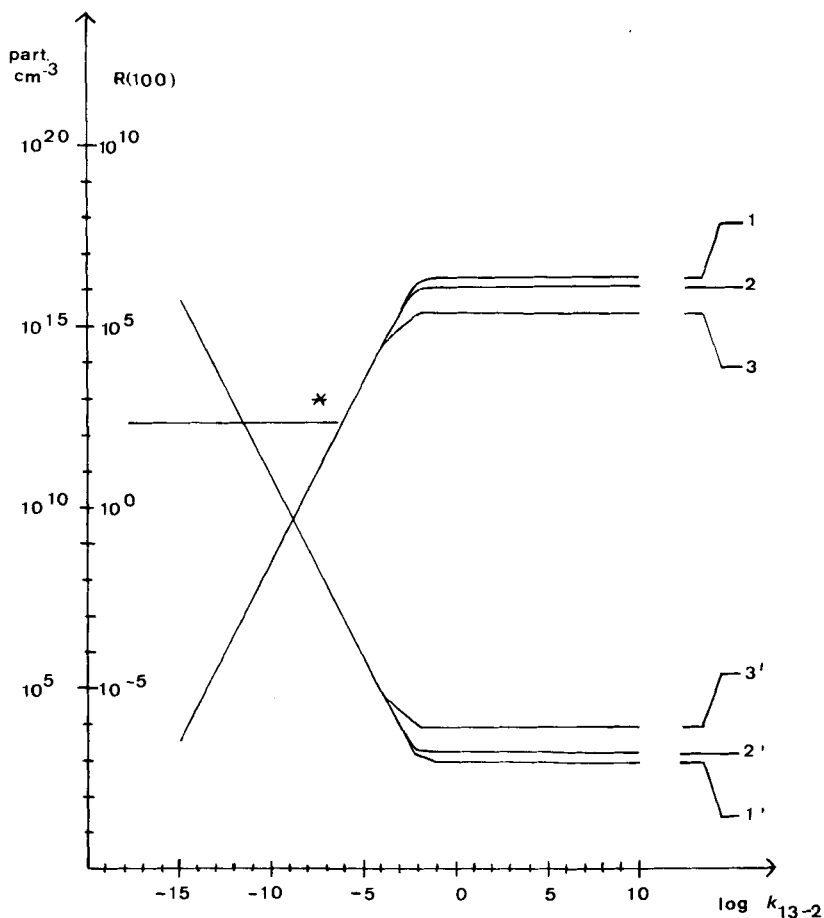


Fig. 5. Gas-phase *cis*-2-butene ozonolysis: kinetic simulation of epoxide formation (s. Schemes 2 and 3, chap. 4.3.1). *: detection limit for 2,3-epoxybutane.

Falling curves: $R(100)$ = ratio of epoxide concentration produced by reactions 0 and 13 after 100 s.

Growing curves: total epoxide concentration (cm^{-3}) produced from biradical V after 100 s.

Initial conditions (LR.-MW.): $p_{\text{O}_3}(0) = p_{\text{C}_4\text{H}_8}(0) = 1 \text{ Torr}$, $p_{\text{Ar}}(0) = 0$.

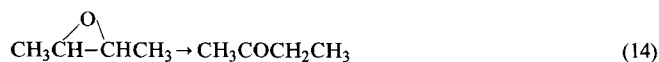
1, 1': particle concentration and $R(100)$, respectively, for $k_{13-2}/k_6 = 10$; 2, 2': for $k_{13-2}/k_6 = 1$; 3, 3': for $k_{13-2}/k_6 = 0.1$.

sequence (2) to (13) appears necessary, requiring k_{13-2} values of the order of at least 10^{-5} s^{-1} . This is likewise demonstrated by the plot of the epoxide concentration (Fig. 5) at $t = 100 \text{ s}$ versus $\log k_{13-2}$. Assuming $A_{13-2} \approx 10^{15} \text{ s}^{-1}$ would imply the value $E_{13-2} \approx 29 \text{ kcal/mol}$, which appears acceptable for the decomposition reactions (13-2).

It should be kept in mind that calculation of the concentration of $\text{O}(^3\text{P})$ by means of the kinetic equations of Scheme 2 leads to an upper limit epoxide production by $\text{O}(^3\text{P})$ addition. As mentioned above it should be kept in mind that O-atoms might be produced by other reactions of the ozonolysis mechanism, e.g. $\text{OH} + \text{O}_3 \rightarrow \text{O} + \text{O}_2 + \text{OH}$, $\text{OH} + \text{OH} \rightarrow \text{O} + \text{H}_2\text{O}$ [56]. A realistic inclusion of these in the epoxide formation mechanism appears difficult at the present time.

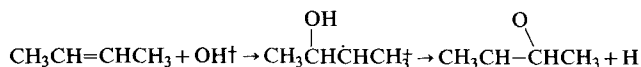
Epoxide production from ethylene ozonolysis has been proven by isotope experiments to occur by a process in which the two C-atoms of the double bond remain connected. Though not yet explicitly demonstrated, the same may rather safely be assumed to hold also for the epoxide production from *cis*-2-butene ozonolysis. This, together with the results of the kinetic modelling, affords strong support for the existence of the biradical intermediate V, proposed as an alternative (or precursor) of the *Criegee* mechanism [7].

The observation of 2-butanone may naturally be explained by isomerization of the 2,3-epoxybutanes:



Isomerization reactions of this type feature activation energies and *A* factors of the order of 50 kcal/mol and 10^{15} s^{-1} , respectively [58] [59]. Efficient conversion to 2-butanone apparently requires non-thermalized epoxide. As shown in *Table 6* (reactions (13), (14), and (15)) formation of the epoxides is exothermic by 30–45 kcal/mol; part of this energy obviously would be required for efficient conversion to 2-butanone. Since the latter reaction will produce the ketone with some 60 kcal/mol excess energy, subsequent decomposition to 3-buten-2-one and a variety of radicals may take place to a considerable extent.

Formation of epoxides might occur from other reactions than those considered above in *Schemes 2* and *3*, e.g. by addition of OH radicals to olefins according to:



Reactions of the OH radical with ethylene have been studied by *Howard* [44] and by *Meagher & Heicklen* [60]. Product analysis yielded no evidence for ethylene oxide formation, however, its isomers $\text{CH}_2=\text{CHOH}$ and CH_3CHO were detected. Therefore, one cannot definitely exclude epoxybutane formation by reaction of *cis*-2-butene with radicals. However, the fact that epoxide formation is definitely proven in LR-MW. experiments in spite of very efficient destruction of OH radicals by wall collisions (*cf.* *Table 3*) renders the OH mechanism rather unimportant.

4.3.2. *The formation of complex products other than epoxides.* The assumption that formation of many of the complex products (except epoxides) involves methyldioxirane (VI) as shown by the *Scheme 1* requires some comment and discussion. In view of the scarcity of available kinetic data the mechanism clearly has to be restricted to simple plausible possibilities, accompanied by thermochemical and thermokinetic estimates. In *Table 6* such data are collected for most steps of *Scheme 1*. The estimates are based on *Benson's* group contribution method [61] and an extension is made for radicals (Appendix I). Since radical mechanisms for olefin ozonolysis have been discussed by numerous authors, most of these are left out in *Scheme 1* but will briefly be mentioned where appropriate. Furthermore, reactions of O_3 with reaction products are taken into consideration to a fragmentary extent only. Some information of this aspect of ozonolysis is available from the work of *Braslawsky & Heicklen* [48].

Table 6. *cis*-2-Butene ozonolysis: thermochemical and kinetic data for complex-product-formation reactions

No. of the reaction ^{a)}	Reaction	ΔH_R° (298) ^{b)} c)	A-Factor ^{d)}	Activation energy kcal/mol	Ref.
2	$\text{CH}_3\text{CHO}_3\text{CHCH}_3(\text{V}') \rightarrow \text{CH}_3\text{CH}(\text{O}_2)\text{CH}(\text{O})\text{CH}_3(\text{V})$	15 ^{e)} 32 ^{f)}	E 14.5	20-50	[54] ^{g)}
6	$\text{CH}_3\text{CH}(\text{O}_2)\text{CH}(\text{O})\text{CH}_3 \rightarrow \text{CH}_3\text{CHO} + \text{CH}_3\text{HCOO}$ $\text{O}-\text{O}$	- 16 ^{e)} - 63 ^{f)} < -9	E 14.5	12	[54]
10	$\text{CH}_3\text{CHO}_3\text{CHCH}_3 \rightarrow \text{CH}_3\text{CHOCHCH}_3(\text{VIII})$ $\text{O}-\text{O}$	- 64			
	$\text{CH}_3\text{HCOO} + \text{CH}_3\text{CHO} \rightarrow \text{CH}_3\text{CHOCHCH}_3$ $\text{O}-\text{O}$	- 61			
10'	$\text{CH}_3\text{CH}(\text{O}_2)\text{CH}(\text{O})\text{CH}_3 \rightarrow \text{CH}_3\text{CHOCHCH}_3$ $\text{O}-\text{O}$	- 32			
13	$\text{CH}_3\text{CH}(\text{O}_2)\text{CH}(\text{O})\text{CH}_3 \rightarrow \text{CH}_3\text{CH}-\text{CHCH}_3 + \text{O}_2$ O	- 78 ^{e)} - 95 ^{f)} $- 27^e) - 44^f)$		50	
14	$\text{CH}_3\text{CH}-\text{CHCH}_3 \rightarrow \text{CH}_3\text{COCH}_2\text{CH}_3$ O	- 27	E 15.5		
15	$\text{CH}_3\text{CH}-\text{CHCH}_3 \rightarrow \text{CH}_3\text{COCH}=\text{CH}_2 + \text{H}_2$ O	0			
6-1	$\text{CH}_3\text{HCOO} \rightarrow \text{CH}_3\text{COOH}(\text{CH}_3\text{COOH}^\dagger)$	- 94	E 14		
6-2	$\text{CH}_3\text{HCOO} \rightarrow \text{CH}_2(\text{OH})\text{CHO}$ $\text{O}-\text{O}$	- 67			
6-3,3'	$\text{CH}_3\text{HCOO} \rightarrow \text{CH}_2-\text{CH}_2(\rightarrow 2 \text{CH}_2\text{O})$ $\text{O}-\text{O}$	+ 9 (-52)	E 14		
6-4	$\text{CH}_3\text{HCOO} \rightarrow \text{HCOOCH}_3$	- 75			
6-5	$\text{CH}_3\text{HCOO} \rightarrow \text{CH}_4 + \text{CO}_2$	- 103			
6-6	$\text{CH}_3\text{HCOO} \rightarrow \text{CH}_3\text{OH} + \text{CO}$	- 65			
6-7	$\text{CH}_3\text{HCOO} \rightarrow \text{CH}_2=\text{C}=\text{O} + \text{H}_2\text{O}$	- 63			
6-8	$\text{CH}_3\text{HCOO} \rightarrow \text{CH}_3\text{CO} + \text{OH}$	+ 13			

6-9	$\square \text{CH}_3\text{HCOO} \rightarrow \text{CH}_3 + \text{CO}_2 + \text{H}$	+ 1
6-10	$\square \text{CH}_3\text{HCOO} \rightarrow \text{CH}_3 + \text{CO} + \text{OH}$	+ 26
6-11	$\square \text{CH}_3\text{HCOO} + \text{CH}_3\text{CHO} \rightarrow \text{CH}_3\text{CHOCHCH}_3 \text{ (VIII)}$	E 10
6-12	$\square \text{CH}_3\text{HCOO} + \text{CH}_3\text{HCOO} \rightarrow \text{H}_2\text{O} + (\text{CH}_3\text{CO})_2\text{O}$	- 32
6-12'	$\square \text{CH}_3\text{HCOO} + \text{CH}_3\text{COOH} \rightarrow \text{H}_2\text{O} + (\text{CH}_3\text{CO})_2\text{O}$	- 178
6-13	$\square \text{CH}_3\text{HCOO} + \text{H}_2\text{O} \rightarrow \text{CH}_3\text{OH} + \text{HCOOH}$	- 86
6-14	$\square \text{CH}_3\text{HCOO} + \text{HCOOH} \rightarrow \text{CH}_3\text{COOCHO} + \text{H}_2\text{O}$	- 71
6-14'	$\square \text{CH}_3\text{HCOO} + \text{CO} \rightarrow \text{CH}_3\text{COOCHO}$	- 83
6-14''	$\text{CH}_2=\text{C}=\text{O} + \text{HCOOH} \rightarrow \text{CH}_3\text{COOCHO}$	- 89
6-15	$\text{CH}_3\text{COOCHO} + \text{HCOOH} \rightarrow \text{CH}_3\text{COOH} + (\text{HCO})_2\text{O}$	- 19
6-16	$\square \text{CH}_3\text{HCOO} + \text{CH}_3\text{HCOO} \rightarrow (\text{CH}_3)_2\text{C}=\text{C}=\text{O} + \text{H}_2\text{O} + \text{O}_2$	0
6-16'	$\square \text{CH}_3\text{HCOO} + \text{CH}_2=\text{CO} \rightarrow (\text{CH}_3)_2\text{C}=\text{C}=\text{O} + \text{O}_2$	- 104
6-17	$\square \text{CH}_3\text{HCOO} + \text{O}_3 \rightarrow \text{CH}_3\text{CO}_3\text{H} + \text{O}_2$	- 6
6-17''	$\square \text{CH}_3\text{HCOO} + \text{HO}_2 \rightarrow \text{CH}_3\text{CO}_3\text{H} + \text{OH}$	- 66

a) Numbering refers to *Scheme 1* and to the mechanistic scheme of ethylene ozonolysis [13].

b) Reaction enthalpy estimate of reaction R.

c) This work.

d) First order reactions: s^{-1} , second order reactions $(\text{mol cm}^{-3})^{-1} \text{s}^{-1}$, E 15 denotes 10^{15} .

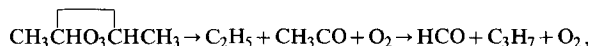
e) Calculated from extended *Benson* group contributions (Appendix D).

f) Calculated from $D(\text{O}-\text{O}) = 38 \text{ kcal/mol}$.

g) Estimates for ethylene ozonolysis.

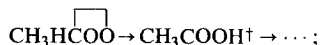
For the discussion the reactions of methyldioxirane (VI) will be grouped into unimolecular rearrangement and decomposition reactions on one hand and bimolecular processes on the other hand.

4.3.2.1. *Products related to V' or V.* Besides formation of the epoxides discussed in 4.3.1, this work yielded little indication for production of complex reaction species directly from either the primary ozonide V' or from the biradical V. Several authors have considered a number of decay modes of these intermediates to produce radicals [5] [6]



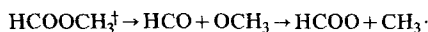
from which further radicals like HO_2 , H, OH^\dagger should be formed. Additional reactions of these have already been briefly mentioned.

4.3.2.2. *Unimolecular reaction modes of methyldioxirane (VI).* Table 6 gives the data of the reactions (6-1) to (6-7), which are either rearrangements or decompositions of VI. Regarding reaction (6), which constitutes a possible path generating VI, it appears probable that VI is formed with excess internal energy. Therefore, even the radical producing reactions (6-8) to (6-10) may be assumed to be kinetically relevant. Processes (6-1) to (6-7) are all highly exothermic and should be taken as possible pathways for production of CH_3COOH , CH_4 , CH_3OH , $\text{CH}_2(\text{OH})\text{CHO}$, H_2CO , HCOOCH_3 , $\text{CH}_2=\text{C}=\text{O}$ and dioxetane. Among these the last three have not been detected. Whereas no explanation for the lack of methyl formate and ketene seems available, the dioxethane is predicted to have a life-time below 0,1 s in our experiments [62] and therefore probably escapes detection by both LR.-IR. and LR.-MW. One also could consider the sequence



however, the production of HCOOCH_3 and $\text{CH}_2=\text{C}=\text{O}$ from thermalized CH_3COOH would be highly endothermic in most instances.

As mentioned earlier, alternative radical mechanisms have been suggested by numerous workers [5] [6] [49], to which the reactions (6-1) to (6-7) form an alternative. Since (6-4) produces highly energized methyl formate it may act as a radical source, e.g.



4.3.2.3. *Bimolecular reactions of methyldioxirane (VI).* By reactions (6-11) to (6-17) (cf. Table 6) a mechanism is suggested by which production of anhydrides, peroxyacetic acid and dimethyl ketene should be explained by bimolecular reactions of VI. Consider first reaction (6-11) leading to the secondary ozonide VIII. This product has been identified in both LR.-IR. and LR.-MW. experiments. Its observation in *cis*-2-butene ozonolysis has been claimed earlier by *De More* [63] and by *Hanst et al.* [64] but escaped detection in recent experiments by *Niki et al.* [11], carried out under conditions where it should have been detectable. The latter authors point out that detection by gas IR. spectroscopy is difficult for ozonides more complex than secondary propene ozonide. This inconsistency prompted us to devote considerable effort to unequivocal identification.

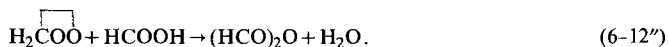
First, for identification in LR.-IR. experiments the mixture of stereoisomeric 2-butene ozonides was synthesized by liquid phase ozonolysis in order to take the reference matrix spectra shown in *Figure 3*. Because of their high resolution and small line width, matrix spectra prove appropriate for unambiguous detection in contrast to gas IR. spectra. Secondly, by means of the synthetic samples the microwave spectral data of the (eq.eq)-conformer were considerably extended. The results of this work are collected in Appendix II and were essential for unequivocal identification of VIII.

Hence by both LR.-IR. and LR.-MW. the formation of VIII in the gas-phase ozonolysis of *cis*-2-butene is undoubtedly proven. Although not yet demonstrated by isotope experiments, it probably is produced *via* sequence (2), (6) and (10) or an analogous route involving *Criegee* intermediates, in which the C-atoms of the C,C double bond are fully separated. This has to be contrasted with the reaction channel generating 2,3-epoxybutanes.

The reactions (6-11) to (6-17) formulated in order to explain production of anhydrides, dimethyl ketene and peracetic acid may be commented on in the following way: (i) For all steps at least one reactant should be present in relatively high concentration, *i.e.* either O₃, VI, acetaldehyde or one of the transformation products of the latter species.

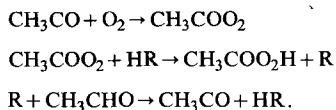
(ii) Almost all steps are highly exothermic, but it appears difficult to either formulate appropriate transition states or to give empirical estimates of particular rate parameters. Kinetic modelling, as a consequence, meets the problem of too many uncertain rate constants and possibly non-thermalized reactants.

(iii) Experiments to enhance reaction (6-14') by addition of CO have not been attempted in this work, but proved negative in ethylene ozonolysis [13]. Accordingly formation of formic anhydride in the latter case might rather be formulated as



Reactions (6-12), (6-14), (6-14'') and (6-15) yield an explanation for the observation of all three anhydrides. As shown in the ethylene case anhydride formation involves reaction (6) or the analogous split into the *Criegee* intermediates, and the same will hold quite probably also for *cis*-2'-butene ozonolysis.

(iv) For the formation of peracetic acid alternatives to (6-17) involving radicals could be responsible, *e.g.*

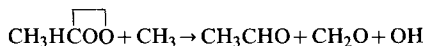
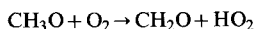
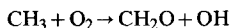
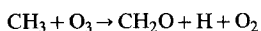


However, it should be mentioned, that oxidation of acetaldehyde by O₃ seems far too slow to contribute noticeably to peroxyacid formation [48].

4.3.2.4. *Relative Product Concentrations.* Obviously the concentration of most of the complex products collected in *Table 3* are quite small in comparison to the observed formaldehyde production. In spite of large uncertainties of the concentration data, a few aspects deserve a comment: (i) the data make obvious that the complex reaction species contribute but little to the overall C-H-O balance, except H₂CO.

(ii) The formaldehyde concentration is estimated to be $2-4 \cdot 10^{16} \text{ cm}^{-3}$. Probably this surprisingly high production cannot be traced back to reaction (6-3/3') alone,

because it is 5–2 times higher than the one of CH_3CHO . Reactions of type (6–3') have often been regarded as a source for chemiluminescent formaldehyde. On the other hand numerous radical reactions for H_2CO production (and similarly destruction) may be suggested [5] [6] [9] [49], e.g.



some of which may contribute to the high yield observed.

(iii) The approximate equality of the concentrations of the stereoisomeric 2-epoxybutanes is in agreement with the assumption made in the kinetic modelling in chap. 4.3.1.

(iv) The relative efficiency of the decomposition modes (13) and (6) of the biradical V may be estimated from the particle concentrations of the 2,3-epoxybutanes and the aldehyde to amount to approx. 10^{-4} . This may afford an explanation for the fact that epoxide formation most often escaped detection. It also gives a demonstration of the high sensitivity and specificity of LR.-MW. spectroscopy.

(v) Provided the mechanism pictured in *Scheme 1* represents the main formation paths of CH_3COOH , CH_3OH , $\text{CH}_2(\text{OH})\text{CHO}$ (and ev. H_2CO), the relative decomposition rates of methyldioxirane to these particles are roughly 1 : 8 : 0.05.

5. Remarks and Conclusion. – The results of this work show that also for the *cis*-2-butene ozonolysis a *Criegee* type mechanism is dominant, but at the same time they give independent support for the existence of a second reaction channel involving the transient biradical V and epoxide formation without breaking the C(2),C(3)-bond. For the biradical V a large number of formally possible abstraction reactions have been suggested by *O'Neal & Blumstein* [7] leading to a variety of hydroperoxy- and hydroxyketones and hydroperoxides. It therefore appears surprising that none of such species has so far been unequivocally identified. However, there is indication in the work of *Atkinson et al.* [5] that complex reaction products of this sort are formed. Furthermore, there are still unidentified lines in LR.-IR. and LR.-MW. reaction spectra.

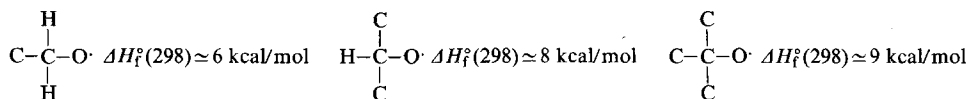
Reviewing the mechanism of ethylene ozonolysis proposed earlier [13] it seems now appropriate to formulate the production of formic anhydride according to reaction (6–12").

Substantiation of the mechanism for complex product formation suggested in this paper requires a complementation by radical reactions and a more complete kinetic modelling. Radical intermediates and reaction rates are to a large extent available from other work. Both LR.-MW. and LR.-IR. should in principle yield also quantitative information about rate constants and products concentration. Work directed to these aims is under way in our laboratory as well as linear-reactor-matrix ESR./ENDOR experiments. The latter technique should allow not only identification of radical intermediates but also provide kinetic data. The

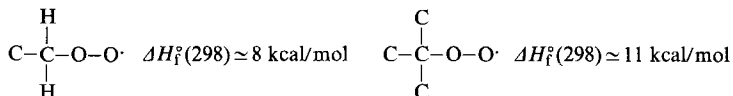
existence of radicals in both ethylene and *cis*-2-butene ozonolysis has recently been demonstrated [65]. Also the central role ascribed to methyldioxirane (VI) should be further investigated. The corresponding homolog dioxirane (VII) and its isomeric and electromeric forms have been the subject of quantum mechanical investigation by *Ha et al.* [66], by *Wadt & Goddard* [67] and by *Hiberty* [68]. In these papers little attention has been paid to transition states lying between dioxirane, its isomers and its decomposition products. However, these would be required to support relevance of the mechanism proposed above. It should also be noted that there are considerable inconsistencies between thermochemical estimates (*cf.* Appendix I) which should be removed by further quantum chemical studies. Work in this direction is in course in our laboratory.

Appendix I. - For the evaluation of thermochemical estimates of reactions involving the biradical V no group contributions seem to be available in literature. Such group increments may be obtained as shown below.

Alkoxy radicals. *Benson* [61] has reported $\Delta H_f^\circ(298)$ values for the radicals $\text{CH}_3\text{O}^\cdot$, $\text{C}_2\text{H}_5\text{O}^\cdot$, *iso*- $\text{C}_3\text{H}_7\text{O}^\cdot$ and *t*- BuO^\cdot to be *ca.* +3.5, -4, -12.6 and -21.6 kcal/mol, respectively. Decomposing these values yields group contributions involving the radical at the oxygen atom:



Peroxyalkyl radicals. From $\Delta H_f^\circ(298)$ estimates for $\text{CH}_3\text{OO}^\cdot$, $\text{C}_2\text{H}_5\text{OO}^\cdot$ and *t*- BuO_2^\cdot [41] one similarly derives the group contributions



Both types of group increments were used in the derivation of the thermochemical estimates in Table 6. It is obvious that these values should be considered as preliminary estimates.

Table 7. Microwave spectrum of the secondary *trans*-(*eq,eq*)-2-butene ozonide

Transition	Transition frequencies [MHz]	
	Obs.	Obs.-calc.
2 (2, 0)-1 (1, 1)	20199.399	-0.010
4 (2, 3)-3 (1, 2)	26336.970	0.047
5 (1, 5)-4 (0, 4)	20309.924	-0.035
6 (0, 6)-5 (1, 5)	20006.986	0.006
6 (1, 6)-5 (0, 5)	23240.238	-0.022
7 (0, 7)-6 (1, 6)	23909.294	0.016
7 (1, 7)-6 (0, 6)	26207.811	-0.000
8 (1, 7)-7 (2, 6)	24043.590	-0.001
8 (3, 6)-8 (2, 7)	22105.895	0.009
11 (3, 9)-11 (2, 10)	25027.882	-0.040
12 (3, 9)-12 (4, 8)	24970.256	-0.002
13 (3, 10)-13 (4, 9)	23767.079	-0.001
14 (1, 13)-14 (2, 12)	23762.600	-0.047
17 (3, 14)-17 (2, 15)	23168.695	-0.068
20 (4, 16)-20 (3, 17)	23357.973	0.048
23 (5, 18)-23 (4, 19)	25629.566	-0.003
24 (5, 19)-24 (4, 20)	26494.976	-0.005

Appendix II. – Molecular species present in low concentrations in a reaction mixture can only be identified successfully from their rotational spectra if the strongest transitions are selected for a search. Often the high J Q-branch transitions are among the strongest transition of a rotational spectrum.

Only a small number of low J transitions up to $J=7$ have been reported from the analysis of the microwave spectrum of the *trans*-(eq,eq)-isomer of the secondary ozonide of 2-butene. Therefore, we considerably extended the assignment including Q-branch transitions up to $J=24$. Seventeen transi-

Table 8. Rotational constants and centrifugal distortion constants of *trans*- $C_4H_8O_3$

A	6022.0553 (95) MHz	Δ_{JK}	–0.014 (131) kHz
B	2103.1359 (68) MHz	Δ_K	2.44 (134) kHz
C	1695.6843 (58) MHz	δ_J	0.0245 (42) kHz
Δ_J	0.086 (66) kHz	δ_K	0.301 (142) kHz

tion frequencies were measured with an accuracy of 20 kHz using a computer controlled microwave spectrometer. They are listed in *Table 7* together with their differences to the calculated values.

The new transition frequencies served as a basis for a least-squares adjustment of the rotational constants and the quartic centrifugal distortion constants. The results are collected in *Table 8*. The standard deviations of the spectroscopic constants from the least-squares fit are given in parentheses. The centrifugal distortion constants are small and not all of them could be determined with sufficient accuracy from the measured set of μ_b transitions. These rotational and centrifugal distortion constants allow accurate predictions of those transition frequencies which have not been measured so far.

REFERENCES

- [1] T. Vrbaski & R. J. Cvetanovic, *Can. J. Chem.* **38**, 1063 (1960).
- [2] Y. K. Wei & R. J. Cvetanovic, *Can. J. Chem.* **41**, 913 (1963).
- [3] B. J. Finlayson, J. N. Pitts, jr. & H. Akimoto, *Chem. Phys. Lett.* **12**, 495 (1972).
- [4] L. A. Hull, I. C. Hisatsune & J. Heicklen, *J. Am. Chem. Soc.* **94**, 4856 (1972).
- [5] R. Atkinson, B. J. Finlayson & J. N. Pitts, jr., *J. Am. Chem. Soc.* **95**, 7592 (1973).
- [6] B. J. Finlayson, J. N. Pitts, jr. & R. Atkinson, *J. Am. Chem. Soc.* **96**, 5356 (1974).
- [7] H. E. O'Neil & C. Blumstein, *Int. J. Chem. Kin.* **5**, 397 (1973).
- [8] R. E. Huie & J. R. Herron, *Int. J. Chem. Kin. Symposium No. 1*, 165 (1975).
- [9] J. T. Herron & R. E. Huie, *J. Am. Chem. Soc.* **99**, 5430 (1977).
- [10] J. T. Herron & R. E. Huie, *Int. J. Chem. Kinet.* **10**, 1019 (1978).
- [11] H. Niki, P. D. Maker, C. M. Sarage & L. P. Breitenbach, *Chem. Phys. Lett.* **46**, 329 (1977).
- [12] R. W. Murray, *Acc. Chem. Res.* **1**, 313 (1968).
- [13] H. Kühne, S. Vaccani, A. Bauder & Hs. H. Günthard, *Chem. Phys.* **28**, 11 (1978).
- [14] H. Ruprecht, Thesis ETH Zurich, to be published.
- [15] Ch. W. Gillies, R. P. Lattimer & R. L. Kuczkowski, *J. Am. Chem. Soc.* **96**, 1536 (1974).
- [16] F. L. Greenwood & H. Rubinstein, *J. Org. Chem.* **32**, 3369 (1967).
- [17] R. P. Lattimer, R. L. Kuczkowski & Ch. W. Gillies, *J. Am. Chem. Soc.* **96**, 348 (1974).
- [18] I. Muramatsu, M. Itoi, M. Tsuji & H. Hagitani, *Bull. Chem. Soc. Jpn.* **37**, 756 (1964).
- [19] D. Garven, *J. Am. Chem. Soc.* **77**, 4161 (1955).
- [20] W. A. Patterson, *Anal. Chem.* **26**, 823 (1954).
- [21] P. Groner, I. Stolkin & Hs. H. Günthard, *J. Phys. E. Sc. Instr.* **6**, 122 (1973).
- [22] H. W. Kroto, 'Molecular Rotation Spectra', J. Wiley and Sons, London 1975, p. 88.
- [23] T. H. Hill, 'Introduction to Statistical Mechanics', Addison-Wesley Publishing Comp., Inc., London 1960, p. 147.
- [24] K. L. Redington, *J. Mol. Spectrosc.* **65**, 171 (1977).
- [25] A. Serrallach, R. Meyer & Hs. H. Günthard, *J. Mol. Spectrosc.* **52**, 94 (1974).
- [26] H. Kühne, T.-K. Ha, R. Meyer & Hs. H. Günthard, *J. Mol. Spectrosc.* **77**, 251 (1979).
- [27] H. Hollenstein, private communication.
- [28] C. V. Berney, R. L. Redington & K. C. Lin, *J. Chem. Phys.* **53**, 1713 (1970).

- [29] J. Cugley, R. Meyer & Hs. H. Günthard, *Chem. Phys.* 18, 281 (1976).
- [30] A. Bauder & P. N. Gosh, unpublished results.
- [31] R. J. Meyers & W. D. Gwinn, *J. Chem. Phys.* 20, 1420 (1952).
- [32] J. Bellet, C. Samson, G. Steenbeckeliers & R. Westheimer, *J. Mol. Struct.* 9, 49 (1971).
- [33] V. Z. Williams, *J. Chem. Phys.* 15, 243 (1947).
- [34] A. Bauder & Hs. H. Günthard, *J. Mol. Spectrosc.* 60, 290 (1976).
- [35] H. Hollenstein & Hs. H. Günthard, *Spectrochim. Acta* 27A, 2060 (1971).
- [36] L. C. Krisher & E. Saegebarth, *J. Chem. Phys.* 54, 4553 (1971).
- [37] C. V. Berney, K. L. Reddington & K. C. Lin, *J. Chem. Phys.* 53, 1713 (1970).
- [38] J. A. Cugley, W. Bossert, A. Bauder & Hs. H. Günthard, *Chem. Phys.* 16, 229 (1976).
- [39] K. M. Marstokk & H. Moellendahl, *J. Mol. Struct.* 5, 205 (1970).
- [40] K. P. Nair & H. D. Rudolph, *J. Mol. Spectrosc.* 48, 571 (1973).
- [41] M. L. Sage, *J. Chem. Phys.* 35, 142 (1961).
- [42] M. R. Emptage, *J. Chem. Phys.* 47, 1293 (1967).
- [43] R. P. Lattimer, R. L. Kuczkowski & W. L. Gillies, *J. Am. Chem. Soc.* 96, 348 (1974).
- [44] C. J. Howard, *J. Chem. Phys.* 66, 4771 (1976).
- [45] A. Eucken, «Lehrbuch der Chemischen Physik», Akadem. Verlagsgesellschaft, Leipzig 1943, Vol. III, p. 343.
- [46] R. C. Evans, 'Crystal Chemistry', University Press, Cambridge 1966, p. 112.
- [47] D. A. Hansen, R. Atkinson & J. N. Pitts, *J. Photochem.* 7, 379 (1977).
- [48] S. B. Braslawsky & J. Heicklen, *Int. J. Chem. Kinet.* 8, 801 (1976).
- [49] F. S. Toby, S. Toby & H. E. O'Neal, *Int. J. Chem. Kinet.* 8, 25 (1976).
- [50] G. L. Pratt, 'Gas Kinetics', Wiley and Sons, Ltd., London 1969, pp. 88, 110.
- [51] S. W. Benson, 'The Foundation of Chemical Kinetics', McGraw-Hill Inc., New York 1960, pp. 154, 222.
- [52] F. J. Lovas & R. D. Suenram, *Chem. Phys. Lett.* 51, 453 (1977).
- [53] R. I. Martinez, R. E. Huie & J. T. Herron, *Chem. Phys. Lett.* 51, 457 (1977).
- [54] S. W. Benson, 'Thermochemical Kinetics', Wiley and Sons, Inc., New York, 1968, p. 173.
- [55] R. J. Cvetanovic, 'Advances in Photochemistry', Interscience Publishers, New York 1963, Vol. 1, p. 115.
- [56] R. Hampson & D. Garvin, 'Reaction Rate and Photochemical Data for Atmospheric Chemistry 1977', NBS Special Publication 513, Washington D.C. 1978.
- [57] S. W. Benson, ref. 54, p. 73.
- [58] S. W. Benson, ref. 54, p. 171.
- [59] S. W. Benson & H. E. O'Neal, 'Kinetic Data of Gas Phase Unimolecular Reactions', NS RDS-NBS 21, Washington, D.C. 1975, p. 266.
- [60] J. F. Meagher & J. Heicklen, *J. Phys. Chem.* 80, 1645 (1976).
- [61] S. W. Benson, ref. 54, p. 178ff.
- [62] K. R. Kopecky, J. E. Filby, C. Mumford, P. A. Lockwood & J. Y. Ding, *Can. J. Chem.* 53, 1103 (1975).
- [63] W. B. De More, *Int. J. Chem. Kinet.* 1, 209 (1969).
- [64] P. L. Hanst, E. R. Stephens, W. E. Scott & R. C. Scott, Symposium on Air Pollution Research, Div. Petr. Chem. 4, Sept. 1959.
- [65] F. Rakoszi & Hs. H. Günthard, *Chem. Phys. Lett.* 67, 173 (1979).
- [66] T.-K. Ha, H. Kühne, S. Vaccani & Hs. H. Günthard, *Chem. Phys. Lett.* 24, 172 (1974).
- [67] W. R. Wadt & W. A. Goddard, *J. Am. Chem. Soc.* 97, 3004 (1975).
- [68] P. C. Hiberty, *J. Am. Chem. Soc.* 98, 6088 (1976).